Jumps in Foreign Exchange Rates and Stochastic Unwinding of Carry Trades*

Makoto Nirei±
Hitotsubashi University
Institute of Innovation Research

Vladyslav Sushko+
University of California Santa Cruz

May 15, 2010

Abstract

We find that tails of the distribution of JPY/USD exchange rate returns are well approximated by an exponentially dampened power-law, suggesting that same mechanism may be responsible for fluctuations in normal times as well as rare crashes. In addition, extreme episodes of yen appreciation are larger and more persistent than episodes of yen depreciation. The asymmetry is magnified and power-law tails are more elongated during times of higher interest rate differential between U.S. and Japan and higher level of VIX indicating that carry trade may be the driver. We propose a model of strategic carry trader behavior that in equilibrium generates exponentially dampened power-law distribution of jumps in foreign exchange along with "up by the stairs down by the elevator" dynamics arising from the assymetries between negative and positive jumps.

JEL Codes: C73, F31, G32

Keywords: Stochastic Games, Herd Behavior, Fat Tails, Foreign Exchange, Financial Risk and Risk Management

---

* We would like to thank Michael Hutchison for making this collaboration possible and for making the data available to us.

± Institute of Innovation Research, Hitotsubashi University 2-1 Naka, Kunitachi, Tokyo 186-8603, Japan; Email: nirei@iir.hit-u.ac.jp; Phone: +81 (42) 580-8417

+ Department of Economics, E2 University of California Santa Cruz, Santa Cruz, CA 95064; Email: vsushko@ucsc.edu; Phone: +1 (859) 420-2576

1 Introduction

Foreign exchange returns of high (low) yield currencies tend to exhibit negative (positive) skewness -- long duration of runs interrupted by abrupt crashes. Understanding the processes behind rare events in foreign exchange markets is important for both risk management and policy making. Brunnermeier et al. (2009) find that yen has exhibited the highest degree of skewness among developed countries' currencies and attribute it to large periodic yen appreciations caused by the unwinding of carry trade[12]. To account for skewness and kurtosis in financial returns they are normally modeled as a stochastic jump diffusion process intended to handle both "normal" and "rare" events simultaneously. Traditionally, it has been assumed that "rare" events augmenting the Brownian motion in returns follow Merton's compound Poisson normal jump process. However, recently Wu (2006) and Bakshi et al. (2008) put forth exponentially dampened power-law as an alternative to Merton's formulation because of it's better ability to match stochastic skewness in financial returns. We find that jumps in the JPY/USD exchange rate are more likely follow an exponentially dampened power-law rather than Merton's compound Poisson process and, given yen's role as a funding currency in carry trade, propose a model of strategic carry trader behavior that in equilibrium generates exponentially dampened power-law in the distribution of jumps.

Carry trade is the suspect because Japanese yen in particular has served as a funding currency for overseas investments because of prolonged "zero interest rate" policy of the Bank of Japan. Figure 1 shows the JPY/USD exchange rate (top) and the U.S.-Japan interest rate differential (2nd from the bottom). In strong violation of the uncovered interest parity (UIP)[3] an increase in the interest rate spread corresponded with dollar appreciation against the yen in late 1999 through 2000 and again from 2004 through 2007[4]. For instance, Ichiue and Koyama (2008) estimate the UIP regression coefficient as low as -2.79 for the yen. Farhi et al. (2009) interpret UIP violations as a compensation to carry traders for the risk of periodic currency crashes, such as a sharp yen appreciation in 2008 following the sub-prime crisis.

[1]Carry trade is a strategy in which an investor borrows in a low interest rate currency and takes a long position in a higher interest rate currency betting that the exchange rate will not change so as to offset the interest rate differential Burnside et al. (2007) and Hochradl and Wagner (2010) document excess returns to carry trade strategies.

[2]In addition, Gagnon and Chaboud (2007) find that prices of deep out-of-money foreign exchange options indicate an overall market hedge against large yen appreciation.

[3]UIP is an ex-ante no-arbitrage condition predicting that excess returns from holding high interest rate currency must be eliminated through an expected depreciation of that currency. Under rational expectations a regression of exchange rate returns on in interest rate differential should yield a coefficient of 1.

[4]An appreciation of the high yield currency is an example of the forward premium puzzle and the violation of the uncovered interest parity (UIP) well documented by Hansen and Hodrick (1980) and Engel (1996).

We focus on time period from Jan 1, 1999 through Feb 1, 2007, thus the 1998 and 2008 crashes are just outside of our sample. We examine daily jumps in JPY/USD exchange rate extracted using a non-parametric method allowing us to test hypothesis regarding the underlying distribution. We find that a compound Poisson normal jump process is strongly rejected in favor of a process that generates power-law tails in the distribution of jumps. Specifically, the data favors exponentially dampened power-law. We also find that positive and negative jumps in JPY/USD exchange rate exhibit asymmetries indicating higher likelihood of large discrete yen appreciations. The asymmetries are more pronounced when the interest rate differential is high. Splitting the sample by the option-implied volatility index VIX, which Brunnermeier et al. (2009) consider an important measure of risk for carry traders, we find that the asymmetries between positive and negative jumps are greater when the level of VIX is high. Furthermore, only yen appreciation jumps tend to occur over consecutive days and exhibit non-linear dependence indicative on non-random variation. Together these finding are consistent with "up by the stairs down by the elevator" dynamics of investment currency in carry trade.

We propose a model of carry trade that generates exponentially dampened power-law distribution of jumps in foreign exchange rates. The methodology is based on Nirei (2006, 2008) work on stochastic herding. Stochastic herding refers to the phenomena of fraction of agents rationally deciding to synchronize their actions after evaluating random pieces of information that they receive. The nature of carry trade makes strategic interactions particularly susceptible to these dynamic because of strategic complementarity and discrete choice in the actions of carry traders (maintain positive position or unwind completely), as pointed out by Plantin and Shin (2008). We develop a simple static version of their model and without parametric assumptions on private information show that the distribution of the aggregate action and the associated discrete price changes (jumps) follow an exponentially dampened power-law. Thus, in our framework, instead of being outliers largest crashes are extreme events within the same power-law tail. Simulations using power-law paramters estimated from the data are able to produce "once in a decade" catastrophic event predicted as an equilibrium outcome of the model. Also, Baysian Markov Chain Monte-Carlo parameter estimations show that the likelihood of a crash rises with higher speculative incetive and uncerainty as proxied by the interest rate differential and the VIX. Hence our model is consistent with Jansen and de Vries (1991) and Longin (1996) who suggest that price fluctuations in normal times and rare market crashes are caused by the same mechanisms.

The paper is organized as follows: section 2 provides data description and describes the non-paramteric methodology of extracting jumps in foreign exchange rate returns based on bi-power variation in realized volatility; section 3 provides summary statistics and time-series properties of jumps making coparison across subsamples of high and low interest rate differential and the VIX; section 4 fits the exponentially dampened power-law to positive and negative jumps and provides a simulation based

on the fitted parameters; section 5 presents a model of stochastic carry trade unwiding that matches stochastic properties of the jump series and provides additional simulations and parameter estimates to check for consistency in the basic relationship between the tails of JPY/USD exchange rate returns and the levels of the interest rate differential and VIX; section 6 concludes.

2 Data and Non-Parametric Estimation of Jumps

2.1 Data

We use intraday JPY/USD exchange rate data from Olsen and Associates. The data was collected from commercial banks by Tenfore and Oanda, and covers the January 1, 1999 to February 1, 2007 time-period. The data consists of the bid and the offer spot exchange rates at the end of every 5-minute interval over every 24-hour period. The quotes are indicative quotes, i.e. not necessarily traded quotes. In addition we construct a daily series of interest rate spread between U.S. and Japan as the difference between the effective federal funds rate and Japan's uncollateralized overnight call rate. Both are publicly avaiable from the Federal Reserve Bank of New York and Bank of Japan respectively. Finally, we obtain daily Chicago Board Options Exchange (CBOE) S&P 500 options implied volatility index (VIX) data from Wharton Research Data Services (WRDS).

The left panel of Figure 2 shows the normal kernel density plot of the JPY/USD exchange rate log-return series from January 1, 1999 through February 1, 2007. The leptokurtic features are apparent, with a fatter negative tail (yen appreciations). The right panel shows the associated quantile-quantile plot against a normal distribution (red line). Again, the negative tail exhibits larger deviation from the normal hypothesis and has a higher number of data points in the extreme range.

2.2 Extracting jumps using bi-power variation

Consider a jump diffusion process for the evolution of foreign exchange rate returns:

$$ds(t) = \mu(t)dt + \sigma(t)dW(t) + \kappa(t)dJ(t) \tag{1}$$

where $s(t)$ is log exchange rate, $\mu(t)$ is drift, $\sigma(t)$ represents stochastic volatility process, and $W(t)$ is standard Brownian motion such that $dW(t) = \sqrt{dt}dz$ with $dz : N(0,1)$. The last term on the right had side represents the stochastic jump process, $\kappa(t)$ is the size of jump at time t and $dJ(t)$ is an indicator of jumps; $dJ(t) = 1$ with some probability and 0 otherwise. At this stage we do not make any parametric assumptions about $\kappa(t)$. Instead we use a non-parametric method of Bi-Power variation of Barndorff-Nielsen (2004) to estimate daily jumps as the difference between the total intra-day realized volatility, $RV_t(\Delta)$, and its continuous component, $BV_t(\Delta)$. $RV_t(\Delta)$ is just the sum of square intraday

discretely sampled Δ -period returns between time 0 and time t. If the intraday data is obtained at 5 minute intervals then $1/\Delta = 288$ is the number of daily data points. Barndorff-Nielsen and Shephard (2004) show that in the limit (as $\Delta \to 0$) realized daily volatility approaches continuously aggregated sum of square returns. Since returns from two adjacent intraday sample points share the persistent volatility but not the sporadic jumps, it follows that bi-power variation provides a reasonable proxy for the persistent component of the volatility:

$$BV_{t+1}(\Delta) \to \int_t^{t+1} \sigma^2(s)ds$$

as $(\Delta) \to 0$.

Since realized volatility, $RV_{t+1}(\Delta)$, and bi-power volatility, $BV_{t+1}(\Delta)$, can be directly calculated from the observed intraday returns, it follows that the jump component can be approximated as the difference of the two:

$$RV_{t+1}(\Delta) - BV_{t+1}(\Delta) \to \sum_{t<s\le t+1} \kappa^2(s) \tag{2}$$

We take additional steps to account for the finite sample bias and in addition to reporting all jumps, we report jumps estimated with $\alpha = 0.05$ and $\alpha = 0.01$ significance level correcting for intraday noise. Choosing to estimate fewer but more probable jumps as opposed to a continuous adjustment amounts to choosing a smaller significance level α associated with critical value Φ_α The details of this procedures are outlined in the appendix.

3 Descriptive Statistics and Time-Series Properties of RV Jumps

Table 1 shows jump summary statistics. Mean absolute values of jumps in yen appreciations are higher for all α ranging between 0.019 and 0.044 compared to 0.16 and 0.36 for jumps in yen depreciations. Negative jumps (appreciations) also exhibit higher kurtosis. The maximum jump in appreciation is 2.959 compared to the maximum jump of 1.482 in yen depreciation. Finally, the bottom row of Table 1 reports Ljung-Box test statistic for white noise. Negative jumps exhibit high degree of serial correlation with the Q-stat in the 133.5 to 161.9 range. Serial correlation is rejected for positive jumps selected using a more restrictive $\alpha = 0.01$ criteria. Overall, Table 1 indicates that jumps in yen appreciation are more rare than jumps in yen depreciation, but tend to be larger in magnitude and occur over several consecutive days.

3.1 Sample split by interest rate differential and VIX

Next we split the sample by the interest rate differential between U.S. and Japan and by the level of VIX focusing on $\alpha = 0.01$ jumps. If carry trade plays a significant role in the stochastic volatility of JPY/USD exchange rate then the contrast between yen appreciation and yen depreciation jumps should be magnified when carry trade activity is high (high interest rate differential) and when overall market uncertainty is high (high level of VIX). Based on the historical time-series in Figure 1 we observe roughly two regimes in the interest rate differential and VIX. Throughout our sample period Japan has maintained a zero-interest rate policy while the dot-com collapse in the U.S. resulted in monetary easing beginning in late 2000 and the differential fell to the level between 1 and 2% where it remained until the FED began raising rates in 2004. Also, the VIX settled at levels below 20 and exhibited a lower volatility beginning in early 2003. Therefore, we select 2% as the cutoff for the interest rate differential and 20 as the cutoff for VIX (dashed lines). Table 2 shows the associated statistics. Mean and maximum values for κ_- (yen appreciation jumps) are higher when interest rate differential is high, 0.124 compared to 0.093 and 1.386 compared to 1.124 respectively. The difference is more pronounced when compared across subsamples split by VIX. When VIX is high κ_- mean and maximum are 0.140 and 1.386 compared to 0.078 and 0.510 when VIX is low respectively. In contrast, κ_+ (yen depreciation jumps) do not exhibit higher mean or maximum when the differential is high and only slightly higher mean when VIX is high, 0.099 compared to 0.082. Also, only yen appreciation jumps exhibit serial correlation. Overall, the comparison of summary statistics for jumps in realized volatility across different levels of the interest rate differential and VIX are consistent with the hypothesis that carry trade plays an important role in the stochastic volatility in JPY/USD.

3.2 Non-linear dependence in Yen appreciation jumps

Next we test for non-linear dependence in the jump series using DBS test named after Brock, Dechert, and Scheinkman (1987). DBS test can be thought of as non-linear counterpart of the Q-test[5]. The test was applied to find evidence of conditional hetersokedasticity in foreign exchange rate returns by Hsieh (1989) who found that nonlinearity in the return series entered through changing volatility. We are able to examine whether descrete changes in realized volatility exhibit non-linearity. The test embeds the time series of $\kappa(t)$ into m-dimensional vectors with overlapping entries. Then computes the spatial correlation among the points in the m-dimensional space which are within tolerance radius ε of each other. Properly adjusted for the sample size, and specially defined mean and variance the correlation

[5]For detail see Brock et al. (1996).

statistic asymptotically follows a standard normal distribution. We select m in the same way as the number of lags for the Q-test. In addition, we parametrize the test to maintain robustness to unusual or unknow distributions of the series: we choose the lolerance radius such that 0.7 of the total number of pairs of points in the sample lie within ε and the *p-values* are computed by bootstrapping based on 1,000 repetitions. Table 2 shows the results[6]. After a minimal correction for itraday noise is employed (such as $\alpha = 0.05$) only yen appreciation jumps exhibit non-linear dependence, which is statistically significant for all m.

Non-linearity may be due to autoregressive conditional heteroskedasticity, that is exchange rate changes are nonlinear stochastic functions of their own past. For instance Lahaye et al. (2010) model foreign exchange rate jumps using Tobit-GARCH. However, this approach also assumes that the magnitude of the jumps follows a lognormal distribution. An alternative explanation of the nonlinear dependence is that these descrete changes in exchange rate returns are purely deterministic processes that only "look" random. To the extent that nonlinearity is one of the indications of chaos a further finding that jumps follow a power-law in the tail would support the second explanation.

4 Power-Law in the Distribution of Jumps

We follow Wu (2006) who proposes to model the Levy density of jump components as an exponentially damped power-law:

$$Pr(\kappa) \propto \begin{cases} \kappa^{-\zeta_+} e^{-\phi_+ \kappa} & , \kappa > 0 \\ |\kappa|^{-\zeta_-} e^{-\phi_- |\kappa|} & , \kappa < 0 \end{cases} \tag{3}$$

This specification is parsimonious enough to nest several families of jump processes. For instance, the values of the power exponent $1 \le \zeta < 3$ favor a power-law tail[7].

In order to examine whether the tail distribution of jumps follows a power-law we follow the methodology of Clauset et al. (2009). For each possible choice of cutoff value for the power-law tail in the distribution of κ, we estimate the power exponent via the maximum likelihood and calculate the Kolmogorov-Smirnov (KS) goodness-of-fit statistic. We then select the minimum cutoff $\kappa_{\min}$ that gives

[6] We also run the DBS test for jump series before separating into positive and negative samples to find strong evidence of non-linear dependence. The results reported in the paper show that the time-series non-linearity comes from yen appreciation jumps.

[7] In a panel study of different currencies Bakshi et al. (2008) estimates parameters of a jump diffusion processes with exponentially dampened power-law. They do not have observations on jumps separately, so they estimates ζ and ϕ for positive and negative jumps as a part of a richer parametrization scheme for the entire return process. Our study is the first to examine the goodness of fit of exponentially damped power-law model to empirical observations of jumps.

the minimum KS-statistic. Figure 3 shows the probability plots for positive and negative jumps for each level of significance, α, on a log-log scale. A Gaussian decay would appear as a concave curvey, however the fitted straight line on the log-log probability plot indicates that distributions of jumps exhibit strong power-law tails.

The top panel of Table 4 shows exponentially dampened power-law parameter estimates for negative jumps at three different significance levels against the two alternatives: Pareto (pure power-law) and lognormal distribution. Given that the distribution parameters are estimated from a relatively small number of observations in the tail we use Bayesian Markov Chain Monte-Carlo (MCMC) method to estimate the fitted parameter uncertainty for the exponentially dampened power-law. Details of this procedure are provided in the appendix.

The log likelihood values indicate that exponentially dampened power-law is the preferred model for all three negative jump series. The estimates of the power-law exponent ζ greater than 1 indicate that the data favors a process that generates high frequency jumps with infinite variation rather than Merton's compound Poisson process. This is confirmed by the rejection of log-normal distribution in a non-nested comparison based on the log likelihood values. The estimates also show that ζ tends to decline further below 3 as only seginificant jumps are selected.

Table 4 and 5 show exponentially dampened power-law parameter estimates for negative (yen appreciation) and positive (yen depreciation) jumps respectively. Once again a compound Poisson jump process is rejected in favor of a model that yields power-law tail. In contrast to the parameter estimates for negative jumps the estimates of the power-exponent ζ are consistently higher tending to the value of 3 instead of 2. Furthermore, the estimates of the exponential rate β tend to decline when more significant jumps are selected. The difference in parameter estimates and in their behavior across jumps of different significance levels indicates that while both negative and positive jumps follow distributions with power-law tails the underlying data generating processes are not the same. This is confirmed by the simulations of $\alpha = 0.05$ jumps shown in Figure 4 with parameters for the exponentially dampened power-law.

The top panel in Figure 4 correspond to the simulated series while the bottom panel displays the empirical observations of jumps. The amplitude in fluctuations is higher for both empirical and simulated series for the negative jumps. The simulation of negative jump series matches the pattern of the data in generating small jump periods punctuated by extreme deviations. This is not the case for the positive jumps. The simulation based on distribution parameter estimates of positive jumps produces a series more even in magnitude, consistent with the lower variability of the observed positive jumps. Based on simulation results we suspect that the underlying data generating process is different for negative and

positive jumps, with negative jumps subject to more extreme fluctuations. Simulations clearly depict the negative skewness of JPY/USD returns. In the following section we propose a model that yields exponentially dampened power-law distribution of discrete yen appreciations as an equilibrium outcome of rational carry trader behavior.

5 Model of Stochastic Unwinding of Carry Trades

The loose fundamental anchoring of foreign exchange rates, also known as the *exchange rate disconnect puzzle* first documented by Mussa (1986) and Flood and Rose (1993), suggests that strategic behavior by traders can play an important role in exchange rate dynamics. Abreu and Brunnermeier (2003) use a continuous time coordination game to show that short-term consideration and actions of other traders can dominate when prices are not well anchored in fundamentals. In their setting a market finally crashes when a critical mass of arbitrageurs synchronizes their trades. Consider a switching strategy, which is a rule of action put forth by Morris and Shin (1998) as part of the global games framework. Under a switching strategy each trader chooses the action based on her best estimate of the fundamental value bearing in mind that other traders are engaged in the same exercise.

Plantin and Shin (2008) model carry trade using the global games approach. They show that the introduction of leverage makes the actions to engage in carry trade strategic complements across traders because leveraged carry trade generates positive funding externality: by entering into a carry transaction traders appreciate the high yield currency effectively reducing funding costs for one another in terms of the funding currency. Furthermore, they show that funding externalities also work in the opposite direction in response to an adverse shock generating “up by the stairs down by the elevator" dynamics.

We build on a simple static version of their model to show that if each carry trader infers other traders' private information only from their actions then episodes of carry unwinding arise endogenously through rational herd behavior. These dynamics arise from the discrete action space of carry traders: either hold on to an existing carry position or unwind completely. This means that both holding and unwinding actions reveal a traders' private information only partially. Then it is rational for each trader to take the actions of others into account along with her own private information when choosing a carry position for the subsequent period. As a result, in Bayes-Nash equilibrium the threshold value of the signal below which carry traders chose to unwind fluctuates endogenously with the actions of other traders giving rise to sudden episodes of "explosive" unwinding. Furthermore, these dynamics are re-enforced by leverage but are present even in the absence of leverage. Thus, our model suggests that the mechanism behind endogenous carry unwinding is stochastic herding by partially informed traders while leverage only serves to strengthen the resulting chain reaction.

5.1 Model analysis

Consider that there are N informed traders indexed by $i = 1,2,\ldots,N$. Each trader can engage in a carry trade where she holds short in yen and long in dollar, and earns an interest differential $\delta \equiv i - i^*$. Suppose that each trader has an existing carry position $k > 1$ and one new addition of fund in yen. The trader can choose a new carry position $k' \in [0, k+1]$.

We assume that the traders are risk neutral and maximize the expected return from the currency position. The carry δ is stochastic. We assume that there are two states of the world, "High" and "Low", and δ takes from two values δ_H and δ_L, depending on the realization of the state, where $\delta_H > 0 > \delta_L$. The trader's return also depends on the rate of change in the value of the collateral, γ. Thus the traders maximize $E(\delta + \gamma)k'$ by choosing k'. Since the traders are risk neutral, the optimal position is either $k' = k+1$ or $k' = 0$. We call the trader's choice $k+1$ as "stay" and 0 as "exit" of the carry trade.

Let m denote the number of exiting traders. We assume that the collateral value depends on the extent of the net outflow of funds from the carry currency. Thus γ is a decreasing function of $mk - N + m$, where mk is the unwound amount of carry trades by exiting traders and $N - m$ is the increase in the carry position by continuing traders. We also assume that gamma is bounded in a small range: $0 < \gamma < |\delta_L|$. Each trader submits to a market maker her supply schedule, namely "stay" or "exit", conditional on m. The market maker then chooses m so that the number of the exiting traders coincides to the chosen m.

Each trader draws a private signal x_i which is correlated with the state. The distribution of x_i is a common knowledge where x_i is drawn from F if the true state is High and from G if the true state is Low. Let f and g denote the density functions of F and G, respectively. We assume that the odds ratio $f(x)/g(x)$ is increasing in x. Namely, F and G satisfy the monotone likelihood ratio property. This assumption implies that a larger value of x conveys the information that it is more likely that the state is High rather than Low.

We conjecture that each trader employs a threshold strategy in which trader i stays in carry ($k' = k+1$) if $x_i > \bar{x}$ and exits ($k' = 0$) otherwise. For a fixed m, a staying trader must be indifferent between stay or exit if she draws a private information at the threshold level $\bar{x}(m)$. Thus $\bar{x}(m)$ must satisfy the indifference condition:

$$E(\delta + \gamma \mid m, x_i = \bar{x}(m)) = 0 \tag{1}$$

Then,

$$(\delta_H + \gamma)\Pr(High|\, x_i = \bar{x}(m), m) + (\delta_L + \gamma)\Pr(Low|\, x_i = \bar{x}(m), m) = 0 \tag{2}$$

where "Pr" denotes a likelihood function. Equivalently, the threshold $\bar{x}$ is determined by the following equation:

$$\log \frac{\Pr(High|\, x_i = \bar{x}(m), m)}{\Pr(Low|\, x_i = \bar{x}(m), m)} = \log \frac{-\delta_L - \gamma}{\delta_H + \gamma} \tag{3}$$

First, we note that:

$$\frac{\Pr(High|\, x_i = \bar{x}(m), m)}{\Pr(Low|\, x_i = \bar{x}(m), m)} = \frac{\Pr(High, x_i = \bar{x}(m), m)}{\Pr(Low, x_i = \bar{x}(m), m)} \tag{4}$$

$$= \frac{\Pr(x_i = \bar{x}(m)\,|High, m)}{\Pr(x_i = \bar{x}(m)\,|Low, m)} \frac{\Pr(m\,|High)}{\Pr(m\,|Low)} \frac{\Pr(High)}{\Pr(Low)} \tag{5}$$

$$= \frac{f(\bar{x}(m))}{g(\bar{x}(m))} \left(\frac{F(\bar{x}(m))}{G(\bar{x}(m))} \right)^m \left(\frac{1 - F(\bar{x}(m))}{1 - G(\bar{x}(m))} \right)^{N-1-m} \theta_0 \tag{6}$$

where θ_0 denotes the prior likelihood ratio, which is the prior belief on High divided by the prior belief on Low state. The term F/G expresses the likelihood ratio inferred by m exiting traders, and the term $(1-F)/(1-G)$ is the likelihood ratio inferred by staying traders. Note that we only count $N-1-m$ staying traders in this term, because the equation is based on the indifference condition for a staying trader and her own information is already included by the term f/g. From this equation, it is straightforward to show the optimality of the threshold rule: only if a trader draws an information greater than the threshold, i.e. $x_i > \bar{x}$, the left hand side of ((3)) exceeds the right hand side due to the MLRP, and thus the trader chooses to stay in carry.

We can show that the traders' choices are strategic complement, in the sense that a trader's exit increases the likelihood of other traders' exits. This amounts to establish that the threshold for the exit $\bar{x}$ is increasing in m. We obtain the following property as in Appendix B:

$$\frac{d\bar{x}}{dm} = \frac{-\log \dfrac{F(\bar{x})}{G(\bar{x})} + \log \dfrac{1-F(\bar{x})}{1-G(\bar{x})} + \dfrac{(\delta_L - \delta_H)(k-1)\gamma'}{-(\delta_H + \gamma)(\delta_L + \gamma)}}{\dfrac{f'(\bar{x}) - g'(\bar{x})}{f(\bar{x})/g(\bar{x})} + m\left(\dfrac{f(\bar{x})}{F(\bar{x}))} - \dfrac{g(\bar{x})}{G(\bar{x})} \right) + (N-1-m)\left(\dfrac{g(\bar{x})}{1-G(\bar{x})} - \dfrac{f(\bar{x})}{1-F(\bar{x})} \right)} \tag{7}$$

$$> 0 \tag{8}$$

Thus, we have shown that the threshold $\bar{x}$ is increasing in m. This implies that the trader's decision exhibits strategic complementarity: when a trader decides to exit, it increases m and then $\bar{x}$, making other traders more likely to exit. Also, the leverage effect is captured by the third term in the numerator increasing the degree of strategic complementarity. Note however, that $\bar{x}$ increases in m even if γ

is zero indicating that leverage only complements pre-existing dynamics.

We now define an equilibrium as a mapping from a profile of realized private information (x_i) to an action profile with m "exits" and $N-m$ "stays", such that the number of traders with $x_i < \bar{x}(m)$ coincides with m for each realization (x_i). The equilibrium notion here is a standard rational expectations equilibrium in a market microstructure with a market maker and traders submitting supply schedules (Vives (2008)).

Next, we characterize the equilibrium by constructing a fictitious tatonnement process, following Nirei (2006, 2008). We imagine that the market maker finds an equilibrium m as follows. At the initial step $s=0$, the market maker starts with $m_{s=0}=0$ and counts the number of traders who would exit according to their supply schedules given the information $m=0$. If no trader exits, then the process stops here and $m=0$ is chosen as an equilibrium. If $n_{s=0}>0$ traders choose to exit, the step is increased to $s=1$, and $m_{s=1}$ is set by $m_s = m_{s-1} + n_{s-1}$. If no traders other than the traders who chose to exit previously decide to exit, then the process stops and $m=m_s$ is chosen as an equilibrium. Otherwise, the step is increased and the process iterates until it stops. Nirei (2006) has shown that this procedure always converges to an equilibrium m, and the selected equilibrium is the smallest among potential equilibria.

The fictitious tatonnement process m_s, $s=0,1,\ldots$, can be embedded to a stochastic process defined in the probability space of the private information profile (x_i). Namely, we can derive the probability distribution of m_{s+1} conditional on m_s before the realization of x_i. It is shown (Nirei (2006)) that n_s follows a branching process in which the number of "children" born by a "parent" in step s follows a binomial distribution with a probability parameter p_s and population $N-m_s$, and if we increase N to infinity, the binomial asymptotically converges to a Poisson distribution with mean $\mu_s = \lim_{N\to\infty} p_s(N-m_s)$.

This property of the fictitious tatonnement process is utilized to characterize the equilibrium. The equilibrium m is the sum of n_s over s, which is the total number of "children" born in the branching process until it stops. Then, we can apply a powerful theorem by Otter (see Harris (1989)). Consider a branching process n_s in which the mean number of children per parent is constant at μ and the initial condition is $n_0=1$. Then the total population $m=\sum_s n_s$ follows a dampened power-law distribution in the tail:

$$\Pr(m \mid m_0 = 1) = C_0 m^{-1.5} e^{-\phi m} \tag{9}$$

for a large m where ϕ is a constant determined by the distribution of the number of children per parent. In our case where the number of children follows a Poisson distribution, we further have $\phi = \mu - 1 - \log \mu$ for the case of $\mu < 1$ (Nirei (2006)). The key parameter for the fluctuation of m is μ. When $\mu \leq 1$, the fictitious tatonnement n_s is a supermartingale, which stops in a finite step and whose total population m is finite with probability one. Equation ((9)) and the relation between ϕ and μ implies that the mean and variance of m is determined by μ. A greater μ decreases ϕ and thus makes the exponential truncation point further in the tail of ((9)). $\mu = 1$ is the critical point at which ((9)) reduces to a pure power law distribution whose mean is indefinite. Thus, we observe that the model is capable of generating a substantial size of fluctuations in m when μ is close to 1. When μ is greater than 1, the fictitious tatonnement is "explosive" and there is a positive probability in which the process does not stop in a finite step. In our finite model, this event corresponds to the case $m = N$.

In our model, μ_s is not constant over the tatonnement step s. However, we can infer the range of μ_s as follows. Suppose that the true state is "Low". For a large N, the mean number of traders who are induced to unwind the carry by observing an additional trader unwinding to the existing unwinding traders m is approximated by:

$$\mu_s : (N - m_s)\, g(\bar{x}(m_s))/(1 - G(\bar{x}(m_s)))(d\bar{x}(m_s)/dm) \tag{10}$$

where $d\bar{x}/dm$ is the increase in the threshold, $g/(1-G)$ is the conditional density at the threshold level, and $N - m_s$ is the number of staying traders at step s. Then,

$$\mu_s = \lim_{N\to\infty} \frac{-\log\dfrac{F(\bar{x}_s)}{G(\bar{x}_s)} + \log\dfrac{1-F(\bar{x}_s)}{1-G(\bar{x}_s)} + \dfrac{(\delta_L - \delta_H)(k-1)\gamma'}{-(\delta_H+\gamma)(\delta_L+\gamma)}}{\dfrac{1}{N-m}\dfrac{f'(\bar{x}_s) - g'(\bar{x}_s)}{f(\bar{x}_s)/(1-G(\bar{x}_s))} + \dfrac{m}{N-m}\left(\dfrac{f(\bar{x}_s)/g(\bar{x}_s)}{F(\bar{x}_s)/(1-G(\bar{x}_s))} - \dfrac{1-G(\bar{x}_s)}{G(\bar{x}_s)}\right) + \dfrac{N-1-m}{N-m}\left(1 - \dfrac{f(\bar{x}_s)/g(\bar{x}_s)}{(1-F(\bar{x}_s))/(1-G(\bar{x}_s))}\right)} \tag{11}$$

where $\bar{x}_s$ is a short-hand for $\bar{x}(m_s)$. For a fixed, finite m_s, we have:

$$\mu_s = \frac{-\log\dfrac{F(\bar{x}_s)}{G(\bar{x}_s)} + \log\dfrac{1-F(\bar{x}_s)}{1-G(\bar{x}_s)} + \dfrac{(\delta_L - \delta_H)(k-1)\gamma'}{-(\delta_H+\gamma)(\delta_L+\gamma)}}{1 - \dfrac{f(\bar{x}_s)/g(\bar{x}_s)}{(1-F(\bar{x}_s))/(1-G(\bar{x}_s))}} \tag{12}$$

Note that:

$$\frac{-\log\frac{F(\bar{x})}{G(\bar{x})}+\log\frac{1-F(\bar{x})}{1-G(\bar{x})}}{1-\frac{f(\bar{x})/g(\bar{x})}{(1-F(\bar{x}))/(1-G(\bar{x}))}}=\frac{\log\frac{f(\bar{x})/g(\bar{x})}{F(\bar{x})/G(\bar{x})}-\log\frac{f(\bar{x})/g(\bar{x})}{(1-F(\bar{x}))/(1-G(\bar{x}))}}{1-\frac{f(\bar{x})/g(\bar{x})}{(1-F(\bar{x}))/(1-G(\bar{x}))}}>1 \tag{13}$$

Thus, the fictitious tatonnement starts out as an explosive process near $m_s/N=0$.

For a range of larger values of m_s, we can characterize μ as follows. Consider an alternative continuum version of our model in which there are a continuum of traders rather than finite N traders. Then, we expect that the equilibrium fraction of exiting traders to be $G(\bar{x})$ by the law of large numbers. Thus, we impose $m/N=G(\bar{x}(m))$ in the expression ((11)). Then:

$$\mu_s\approx\frac{-\log\frac{F(\bar{x})}{G(\bar{x})}+\log\frac{1-F(\bar{x})}{1-G(\bar{x})}+\frac{(\delta_L-\delta_H)(k-1)\gamma'}{-(\delta_H+\gamma)(\delta_L+\gamma)}}{\frac{f(\bar{x})/g(\bar{x})}{F(\bar{x})/G(\bar{x})}-\frac{f(\bar{x})/g(\bar{x})}{(1-F(\bar{x}))/(1-G(\bar{x}))}} \tag{14}$$

We note that:

$$\frac{-\log\frac{F(\bar{x})}{G(\bar{x})}+\log\frac{1-F(\bar{x})}{1-G(\bar{x})}}{\frac{f(\bar{x})/g(\bar{x})}{F(\bar{x})/G(\bar{x})}-\frac{f(\bar{x})/g(\bar{x})}{(1-F(\bar{x}))/(1-G(\bar{x}))}}=\frac{\log\left(\frac{f(\bar{x})/g(\bar{x})}{F(\bar{x})/G(\bar{x})}\right)-\log\left(\frac{f(\bar{x})/g(\bar{x})}{(1-F(\bar{x}))/(1-G(\bar{x}))}\right)}{\frac{f(\bar{x})/g(\bar{x})}{F(\bar{x})/G(\bar{x})}-\frac{f(\bar{x})/g(\bar{x})}{(1-F(\bar{x}))/(1-G(\bar{x}))}} \tag{15}$$

This expression takes a value greater than 1 when $\bar{x}$ is small (and thus m is small) whereas it takes a value less than 1 when $\bar{x}\to\infty$ (and thus $m\to N$). Thus, we can infer that μ_s travels from an explosive region to a dampening region (if k is small enough) as the fictitious tatonnement develops into a larger m. This suggests that the tatonnement generates m smaller than N when N is large enough, and the fluctuation of m follows the dampened power-law distribution.

The function $\gamma(mk-N+m)$ is constructed so that the dynamic pattern of exchange rates matches with the model when the static equilibrium of the model is repeated with evolving currency position k. Consider the case $k_0=0$. Then the effect of γ on μ in ((11)) is negative, and thus we expect a high probability for staying behavior: $k'=1$. In the next period, we set $k_1=k'=1$. We have a greater value of μ_s, and expect some probability of collective unwinding. When k becomes quite large, we expect an even higher probability of sudden unwinding because of a greater μ_s. Thus, we expect a small value of m and a gradual increase of k over periods, whereas the development of the carry accumulation is punctuated by a “sudden fall" when m takes some large positive value. In terms of the exchange rate, the currency appreciation γ is a negative function of $mk-N+m$, and thus the dynamics of m corresponds to the appreciation by the stairs and the fall by an elevator.

5.2 Correspondence with the data

The model predicts the power exponent of 1.5 in the exponentially dampened power-law. Our empirical estimates for the exponent, conditional on the cutoff value for the tail selected based on the best fit for the Pareto distribution, have yielded estimates of the exponent in the neighborhood of 2. This gap may be rectified by modifications on estimation and modeling. Table 8 illustrates that under alternative selection for the cutoff, κ_{min}, estimates of 1.5 are for ζ are also within the feasible range. The lower cutoff on the tail observations has been selected as one standard deviation in the empirical jump data. Under this more inclusive specification the power-law exponent is 1.527 for negative jumps and 1.495 for positive jumps.

Alternatively, it is known that the power exponent ζ derived in the model is increased above 1.5 if the parameter μ is taken gradually from below the criticality $\mu < 1$ toward the criticality during the time span of observations. This mechanism is called a “sweeping" of control parameter towards a critical point (Sornette(2006)). Recall the case in which we repeat the static equilibrium over periods where the currency position k_t is updated over the periods. When k is small, the tatonnement is likely to be subcritical with $\mu < 1$, while μ is increased toward 1 as k increases and thus the effect of possible sudden appreciation due to the collective unwinding becomes more significant on the overall return of the carry trade. If our data is generated by such process, the situation exactly falls in the scenario of the sweeping of parameter where the key parameter μ gradually sweeps toward the criticality. In this case, the observed jumps exhibit dampened power law with exponent greater than 1.5. The exact value of the exponent depends on how the parameter μ is increased over periods.

At the criticality $\mu = 1$, the model generates a pure power-law distribution for m. The top panel of Figure 5 shows data simulated using a power-law fit to the negative jump series. The simulation approximates the general amplitude in the fluctuations of the empirical data shown in the bottom panel except for the one “catastrophic" event when the simulated jump exceeds 11 in absolute value. This simulation illustrates the ability of the model to incorporate “rare" disasters in the same data generating process.

Whether the rare instances of large jumps in JPY/USD exchange rate are related to carry trade activity is better understood by examing how the paramter values governing the tails change with the level of the interest rate differential and the VIX. Table 7 shows distribution parameter estimates for subsamples of high and low interest rate differentials based on the same 2% cutoff. The power exponent for yen appreciation jumps is 2.007 when the differential is high compared to 2.394 when it is low. In addition, lower ϕ during higher interest rate differential period indicates exponential truncation point

further in the tail of the distribution. intuitively, this means a larger adjustment is induced by the same size shock, or that a larger number of traders m would have switched their strategies before the tatonnement process is completed. Table 8 shows distribution parameter estimates for subsamples split by the level of VIX based on the same 20 point cutoff. When uncertainty is high then exponentially dampened power-law has higher log likelihood than a simple Pareto with a considerably lower estimate of ϕ compared to when VIX is low (0.620 versus 3.327). The negative relationship between ϕ and the ineterest rate differential and the VIX is confirmed by conducting a Bayesian MCMC simulatation of the following hierarchical model:

$$Pr(\kappa_j) \propto \kappa_j^{-1.5} e^{-\phi_j \kappa_j} \; ; \; \kappa_j \in (\kappa_{j,+}, \kappa_{j,-}) \tag{19}$$

where parameter ϕ is assumed to be a linear function of either $(i^{US} - i^{JP})$ or of the VIX:

$$log(\phi_j) = \gamma_0 + \gamma_1 \times (i_j^{US} - i_j^{JP}) + \varepsilon_j \; ; \; j = 1,..,J \tag{20}$$

or

$$log(\phi_j) = \gamma_0 + \gamma_1 \times log(VIX_j) + \varepsilon_j \; ; \; j = 1,..,J \tag{21}$$

with priors $\gamma_0 \sim N(\mu_0, \sigma_0)$, $\gamma_1 \sim N(\mu_1, \sigma_1)$, $\varepsilon \sim N(0, \tau_\varepsilon)$, and $\tau_\varepsilon \sim Gamma(\alpha_\varepsilon, \beta_\varepsilon)$. The τ_ε represents the precision of the random effects term in the model. The hyper-parameters for γ_0 and γ_1 selected such that prior means match the MLE estimates. Table 9 shows the estimation results. The association between the speed, ϕ, of exponential truncation of the tail of jump distribution for both positive and negative jumps is decreasing (that is the branching process depicted by model's μ is intensifying) in the differential and the VIX. Intuitively, stochastic volatility in the JPY/USD foreign exchange market rises (that is tail of the return series are more elongated) when speculative motive is higher, as proxied by the interest rate differential, and when market uncertainty is higher, as measured by VIX. The coefficient γ_1 is statistically significant for both yen appreciation and yen depreciation jumps under the assumption the the generated data is approximately Gaussian. Figures 6 and 7 show the density plots, simulation quantiles, and autocorrelation plots for γ_1 coefficients on the differential and the VIX respectively. A bell curve indicates that a normal approximation to the standard errors in not unreasonable and fact declining ACF plots indicate a good mixture. Overall, we have provided some evidence that parameters governing stochastic volatility in JPY/USD are consistent with the model of herding induced by carry trade opportunities.

6 Conclusion

This paper examines a mechanism that generates tail events in the distribution of foreign exchange returns. We find that jumps in daily returns of JPY/USD over the period from January 1, 1999 through February 1, 2007 are more likely to follow an exponentially dampened power-law than Merton's compound Poisson process. Our data does not include “extreme" episodes in JPY/USD return volatility corresponding to the 1998 LTCM collapse and the 2008 sub-prime crisis, yet exponentially dampened power-law parameter estimates indicate that the data favors a distribution that generates jumps with unbounded variation, essentially attributing rare market crashes and normal return volatility to the same underlying mechanism. In addition, we find that yen appreciation (negative) and yen depreciation (positive) jumps are assymetric: appreciation jumps are more rare, exhibit higher variability, and have higher mean and maximum value. These asymmetries are more pronounced when interest rate differential between the two countries is higher and when market uncertainty is higher (as proxied by VIX). Furthermore, only the negative jumps exhibit autocorrelation and non-linear dependence indicating that episodes of discrete yen appreciations tend to take place over several consecutive days and may be non-random. The asymmetries and higher negative skew of JPY/USD returns are confirmed by simulations based on estimated distribution parameters. We think that such asymmetries are related to the role of yen as a funding currency in carry trade during our sample period since only yen appreciations would have been costly to carry traders producing different dynamics on the way up than on the way down.

We build on a simple static version of Plantin and Shin (2006) carry trade model in which traders follow a switching strategy. We show that if each carry trader infers other traders' private information only from their actions then episodes of “explosive" carry unwinding arise endogenously via a stochastic herding mechanism because of a non-linear dependence of the switching threshold on the actions of others. In Bayes-Nash equilibrium the distribution of the number of traders unwinding their positions fluctuates according to an exponentially dampened power-law and, with a linear price impact function, so do the jumps in foreign exchange returns. The model yields a power-law exponent of -1.5 in the density function of jumps which is found to be in the feasible range of our empirical estimates. Thus, our model incorporates “rare" disasters in the same data generating process as stochastic volatility on day to day basis. In addition the model shows that leverage exacerbates the chain reaction in the carry unwinding but the underlying dynamics are generated by the propensity of carry traders to herd even in the absence of leverage.

References

Abreu, D. and Brunnermeier, M. (2003), Bubbles and crashes, *Econometrica* , Vol. 71, pp. 173-204.

Andersen, T. G., Bollerslev, T. and Diebold, F. X. (2007), Roughing it up: Including jump components in the measurement, modeling, and forecasting of return volatility, The *Review of Economics and Statistics*, Vol. 89, pp. 701-720.

Arnold, B. C. and Press, S. J. (1983), Bayesian inference for pareto populations, *Journal of Econometrics*, Vol. 21, pp. 287 - 306.

Bakshi, G., Carr, P. and Wu, L. (2008), Stochastic risk premiums, stochastic skewness in currency options, and stochastic discount factors in international economies, *Journal of Financial Economics* , Vol. 87, pp. 132-156.

Barndorff-Nielsen, O. E. (2004), Power and bipower variation with stochastic volatility and jumps, *Journal of Financial Econometrics* , Vol. 2, pp. 1-37.

Barndorff-Nielsen, O. E., Graversen, S. E., Jacod, J. and Shephard, N. (2006), Limit theorems for bipower variation in financial econometrics, *Econometric Theory* , Vol. 22, pp. 677-719.

Barndorff-Nielsen, O. E. and Shephard, N. (2006), Econometrics of testing for jumps in financial economics using bipower variation, *Journal of Financial Econometrics* , Vol. 4, pp. 1-30.

Brock, W. A., Scheinkman, J. A., Dechert, W. D. and LeBaron, B. (1996), A test for independence based on the correlation dimension, *Econometric Reviews* , Vol. 15, pp. 197-235.

Brunnermeier, M. K., Nagel, S. and Pedersen, L. H. (2009), Carry trades and currency crashes, *NBER Macroeconomic Annual*, Vol. 23 (1), pp. 313-348.

Burnside, C., Eichenbaum, M. and Rebelo, S. (2007), The returns to currency speculation in emerging markets, *American Economic Review* , Vol. 97, pp. 333-338.

Candelon, B. and Straetmans, S. (2006), Testing for multiple regimes in the tail behavior of emerging currency returns, *Journal of International Money and Finance*, Vol. 25, pp.1187-1205.

Clauset, A., Shalizi, C. R. and Newman, M. E. J. (2009), Power-law distributions in empirical data, *SIAM Review* , Vol. 51, p. 661.

Engel, C. (1996), The forward discount anomaly and the risk premium: A survey of recent evidence, *Journal of Empirical Finance* , Vol. 3, pp. 123-192.

Farhi, E., Fraiberger, S. P., Gabaix, X., Ranciere, R. and Verdelhan, A. (2009), Crash risk in currency markets, *NBER Working Papers* 15062, National Bureau of Economic Research,Inc.

Flood, R. P. and Rose, A. K. (1993), Fixing exchange rates: A virtual quest for fundamentals, *NBER Working Papers* 4503, National Bureau of Economic Research, Inc.

Gagnon, J. E. and Chaboud, A. P. (2007), What can the data tell us about carry trades in japanese yen?, *International Finance Discussion Papers*, 899, Board of Governors of the Federal Reserve System

Hansen, L. P. and Hodrick, R. J. (1980), Forward exchange rates as optimal predictors of future spot rates: An econometric analysis, *Journal of Political Economy* , Vol. 88, pp. 829-53.

Harris, T. E. (1989), *The Theory of Branching Processes*, Dover, NY.

Hochradl, M. and Wagner, C. (2010), Trading the forward bias: Are there limits to speculation?, *Journal of International Money and Finance* , Vol. 29, pp. 423 - 441.

Hsieh, D. A. (1989), Testing for nonlinear dependence in daily foreign exchange rates, *The Journal of Business*, Vol. 62, The University of Chicago Press, pp. 339-368.

Ichiue, H. and Koyama, K. (2008), Regime switches in exchange rate volatility and uncovered interest rate parity, *Working paper series, Bank of Japan*.

Jansen, D. W. and de Vries, C. G. (1991), On the frequency of large stock returns: Putting booms and busts into perspective, *The Review of Economics and Statistics* , Vol. 73, pp. 18-24.

Lahaye, J., Laurent, S. and Neely, C. J. (2010), Jumps, cojumps and macro announcements, *Journal of Applied Econometrics*, Vol. forthcoming.

Longin, F. M. (1996), The asymptotic distribution of extreme stock market returns, *Journal of Business*, Vol. 69, pp. 383-408.

Morris, S. and Shin, H. S. (1998), Unique equilibrium in a model of self-fulfilling currency attacks, *American Economic Review*, Vol. 88, pp. 587-97.

Mussa, M. (1986), Nominal exchange rate regimes and the behavior of real exchange rates: Evidence and implications, *Carnegie-Rochester Conference Series on Public Policy*, Vol. 25, pp. 117-214.

Nirei, M. (2006), Threshold behavior and aggregate fluctuation, *Journal of Economic Theory, Vol. 127, pp. 309-322.*

Nirei, M. (2008), Self-organized criticality in a herd behavior model of financial markets, *Journal of Economic Interaction and Coordination*, Vol. 3, pp. 89-97.

Plantin, G. and Shin, H. S. (2008), Carry trades and speculative dynamics, Working papers, London Business School and Princeton University.

Quintos, C. , Fan, Z. and Phillips, P. (2001),Structural Change Tests in Tail Behaviour and the Asian Crisis, *Review of Economic Studies*, Vol. 68, pp. 633-63.

Sornette, D. (2006), *Critical Phenomena in Natural Sciences*, second edition, Springer.

Vives, X. (2008), *Information and Learning in Markets*, Princeton University Press.

Wu, L. (2006), Dampened power law: reconciling the tail behavior of financial security returns, *Journal of Business*, Vol. 78, pp. 1445-1473.

Appendix

A. Empirical Methodology

A.1 Jump component

In the limit (as $\Delta \to 0$) realized daily volatility approaches continuously aggregated sum of square returns:

$$RV_{t+1}(\Delta) \to \int_t^{t+1} \sigma^2(s)ds + \sum_{t<s\le t+1} \kappa^2(s) \tag{A.1}$$

and $BV_t(\Delta)$ is defined as the sum of the product of adjacent absolute intraday returns standardized by a constant:

$$BV_t(\Delta) \equiv \mu^{-2} \sum_{j=2}^{1/\Delta} | r_{t+j\Delta,\Delta} | | r_{t+(j-1)\Delta,\Delta} | \tag{A.2}$$

where $\mu \equiv (2/\pi)^2$ is the mean of the absolute value of standard normally distributed random variable. Since returns from two adjacent time periods share the persistent volatility but not the sporadic jumps, it follows from (A.2) that bi-power variation provides a reasonable proxy for the persistent component of the volatility. Barndorff-Nielsen et al. (2006) show that:

$$BV_{t+1}(\Delta) \to \int_t^{t+1} \sigma^2(s)ds \tag{A.3}$$

as $(\Delta) \to 0$.

Since realized volatility, $RV_{t+1}(\Delta)$, and bi-power volatility, $BV_{t+1}(\Delta)$, can be directly calculated from the observed asset prices, it follows that the jump component can be approximated as the difference of the two:

$$RV_{t+1}(\Delta) - BV_{t+1}(\Delta) \to \sum_{t<s\le t+1} \kappa^2(s) \tag{A.4}$$

Because of a finite sample the estimate of the squared jump process might be negative so the measure us truncated at zero to get:

$$\kappa_{t+1}(\Delta) \equiv max[RV_{t+1}(\Delta) - BV_{t+1}(\Delta), 0] \tag{A.5}$$

We select only significant jumps while discounting smaller jumps as a part of continuous process or noise. Andersen et al. (2007) derive an asymptotically standard-normally distributed test statistic based on the fourth moment of the jump-diffusion process:

$$Z_{t+1}(\Delta) \equiv \Delta^{1/2} \frac{[RV_{t+1}(\Delta) - BV_{t+1}(\Delta)]RV_{t+1}(\Delta)^{-1}}{[(\mu^4 + 2\mu^2 - 5)max\{1, TQ_{t+1}(\Delta)BV_{t+1}(\Delta)^{-2}\}]^{1/2}} \tag{A.6}$$

where,

$$TQ_{t+1}(\Delta) \equiv \Delta^{-1}\nu^{-3}\sum_{j=3}^{1/\Delta} | r_{t+j\Delta,\Delta} |^{4/3} | r_{t+(j-1)\Delta,\Delta} |^{4/3} | r_{t+(j-2)\Delta,\Delta} |^{4/3} \quad (A.7)$$

$$\nu \equiv 2^{2/3}\Gamma(7/6)\Gamma(1/2)^{-1} \quad (A.8)$$

so that $TQ_{t+1}(\Delta) \to \int_t^{t+1} \sigma^4(s)ds$ as $\Delta \to 0$.

Hence, choosing to estimate fewer but larger jumps amounts to choosing a smaller significance level α associated with critical value Φ_α to compute:

$$\kappa_{t+1,\alpha}(\Delta) = I[Z_{t+1}(\Delta) > \Phi_\alpha] \cdot [RV_{t+1}(\Delta) - BV_{t+1}(\Delta)] \quad (A.9)$$

In addition to reporting all jumps, we report jumps estimated with $\alpha = 0.05$ and $\alpha = 0.01$. As a final step of implementing (A.9). Andersen et al. (2007) tackle first order autocorrelation due to microstructure noise by dividing $BV_{t+1}(\Delta)$ and $TQ_{t+1}(\Delta)$ by $(1-2\Delta)$ and $(1-4\Delta)$ respectively and adjusting the lags on returns.

A.2 Bayesian MCMC Estimation of ζ and ϕ

Under the assumption of exponentially dampened power-law for $\kappa_j \geq \kappa_{min}$ using equation (3) the joint likelihood is:

$$f(\kappa_1, \kappa_2, .., \kappa_J) \propto \prod_{j=1}^{J} \kappa_j^{-\zeta} exp\{-\phi\kappa_j\} \quad (A.10)$$

The conjugate prior families for the power exponent and exponential decay parameter are Gamma families[8]: ζ :*Gamma* $(\alpha_\zeta, \beta_\zeta)$ and ϕ :*Gamma* $(\alpha_\phi, \beta_\phi)$. Combining prior parameter densities with equation (A.10) and assuming ζ and ϕ are orthogonal we obtain the joint posterior:

$$f(\zeta, \phi \mid \kappa_1, \kappa_2, .., \kappa_J) \propto \left[\prod_{j=1}^{J} \kappa_j^{-\zeta}\right] \zeta^{\alpha_\zeta - 1} exp\{-\beta_\zeta \zeta\} \left[exp\left\{-(\sum_{j=1}^{J} \kappa_j + \beta_\phi)\phi\right\}\right] \phi^{\alpha_\phi - 1} \quad (A.11)$$

From (A.11) we obtain complete parameter conditionals:

$$f(\zeta \mid \kappa_1, \kappa_2, .., \kappa_J) \propto \zeta^{\alpha_\zeta - 1} exp\left\{-(\beta_\zeta + \sum_{j=1}^{J} ln(\kappa_j))\zeta\right\} \quad (A.12)$$

and

$$f(\phi \mid \kappa_1, \kappa_2, .., \kappa_J) \propto \phi^{\alpha_\phi - 1} exp\left\{-(\beta_\phi + \sum_{j=1}^{J} \kappa_j)\phi\right\} \quad (A.13)$$

From (A.12) and (A.13)it follows that we can apply the Gibbs step in the MCMC algorithm to sample the power exponent and the exponential decay parameter from the following distributions

[8] See Arnold and Press (1983) for the detailed discussion on the Bayesian techniques to estimate parameters in the power-law distribution

respectively: $$\zeta \mid \kappa_1, \kappa_2, .., \kappa_J \sim Gamma\ (\alpha_\zeta, \beta_\zeta + \sum_{j=1}^{J} ln(\kappa_j)) \tag{A.14}$$

$$\phi \mid \kappa_1, \kappa_2, .., \kappa_J \sim Gamma\ (\alpha_\phi, \beta_\phi + J\bar{\kappa}) \tag{A.15}$$

For each jump sample we have a strong prior for the parameters based on preliminary MLE results, therefore we chose prior parameters such that $\alpha_\zeta/\beta_\zeta = \hat{\zeta}_{MLE}$ and $\alpha_\phi/\beta_\phi = \hat{\phi}_{MLE}$.

B. Derivation of Equation (7)

By taking a partial derivative with respect to m for a fixed $\bar{x}$, we have:

$$\frac{\partial}{\partial m}\log\frac{\Pr(High \mid x_i = \bar{x}, m)}{\Pr(Low \mid x_i = \bar{x}, m)} = \log\frac{F(\bar{x})}{G(\bar{x})} - \log\frac{1-F(\bar{x})}{1-G(\bar{x})} < 0 \tag{B.1}$$

where the inequality obtains because of $F/G < f/g < (1-F)/(1-G)$ since f/g is increasing. Thanks to the MLRP, we also have the following properties:

$$\frac{\partial}{\partial \bar{x}}\log\frac{f(\bar{x})}{g(\bar{x})} > 0 \tag{B.2}$$

$$\frac{\partial}{\partial \bar{x}}\log\frac{F(\bar{x})}{G(\bar{x})} = \frac{g(\bar{x})}{F(\bar{x})}\left(\frac{f(\bar{x})}{g(\bar{x})} - \frac{F(\bar{x})}{G(\bar{x})}\right) > 0 \tag{B.3}$$

$$\frac{\partial}{\partial \bar{x}}\log\frac{1-F(\bar{x})}{1-G(\bar{x})} = -\frac{g(\bar{x})}{1-F(\bar{x})}\left(\frac{f(\bar{x})}{g(\bar{x})} - \frac{1-F(\bar{x})}{1-G(\bar{x})}\right) > 0 \tag{B.4}$$

Then, the partial derivative of the left-hand side of ((3)) with respect to $\bar{x}$ becomes:

$$\frac{\partial}{\partial \bar{x}}\log\frac{\Pr(High \mid x_i = \bar{x}, m)}{\Pr(Low \mid x_i = \bar{x}, m)} = \frac{\partial}{\partial \bar{x}}\log\frac{f(\bar{x})}{g(\bar{x})} + m\frac{\partial}{\partial \bar{x}}\log\frac{F(\bar{x})}{G(\bar{x})} + (N-1-m)\frac{\partial}{\partial \bar{x}}\log\frac{1-F(\bar{x})}{1-G(\bar{x})} > 0 \tag{B.5}$$

The partial derivative of the right-hand side of ((3)) is:

$$\frac{\partial}{\partial m}\log\frac{-\delta_L - \gamma}{\delta_H + \gamma} = \frac{(\delta_L - \delta_H)(k-1)\gamma'}{-(\delta_H + \gamma)(\delta_L + \gamma)} > 0 \tag{B.6}$$

Collecting terms, we obtain:

$$\frac{d\bar{x}}{dm} = \frac{-\log\frac{F(\bar{x})}{G(\bar{x})} + \log\frac{1-F(\bar{x})}{1-G(\bar{x})} + \frac{(\delta_L - \delta_H)(k-1)\gamma'}{-(\delta_H + \gamma)(\delta_L + \gamma)}}{\frac{\partial}{\partial \bar{x}}\log\frac{f(\bar{x})}{g(\bar{x})} + m\frac{\partial}{\partial \bar{x}}\log\frac{F(\bar{x})}{G(\bar{x})} + (N-1-m)\frac{\partial}{\partial \bar{x}}\log\frac{1-F(\bar{x})}{1-G(\bar{x})}} \tag{B.7}$$

$$= \frac{-\log\frac{F(\bar{x})}{G(\bar{x})} + \log\frac{1-F(\bar{x})}{1-G(\bar{x})} + \frac{(\delta_L - \delta_H)(k-1)\gamma'}{-(\delta_H + \gamma)(\delta_L + \gamma)}}{\frac{f'(\bar{x}) - g'(\bar{x})}{f(\bar{x})/g(\bar{x})} + m\left(\frac{f(\bar{x})}{F(\bar{x}))} - \frac{g(\bar{x})}{G(\bar{x})}\right) + (N-1-m)\left(\frac{g(\bar{x})}{1-G(\bar{x})} - \frac{f(\bar{x})}{1-F(\bar{x})}\right)} \tag{B.8}$$

which is strictly positive by the inequalities shown above.

Tables and Figures

Table 1: Summary statistics for realized volatility jumps in JPY/USD exchange rate

	Yen Appreciation Jumps			Yen Depreciation Jumps		
	κ_-	$\kappa_-(\alpha=0.05)$	$\kappa_-(\alpha=0.01)$	κ_+	$\kappa_+(\alpha=0.05)$	$\kappa_+(\alpha=0.01)$
Prop.	47.40%	24.60%	17.20%	48.50%	23.90%	16.70%
Obs.	1255	650	455	1276	628	438
Mean	0.044	0.026	0.019	0.036	0.022	0.016
St. Dev.	0.113	0.097	0.073	0.079	0.068	0.055
Skew.	10.543	14.290	8.575	6.521	8.803	7.876
Kurt.	202.355	351.193	110.709	77.961	133.712	105.325
Min.	0.000	0.000	0.002	0.000	0.000	0.001
Max.	2.959	2.959	1.386	1.482	1.482	1.125
Q-stat	161.899***	79.366***	133.528***	38.296***	33.733***	3.828

Note: All jumps and jumps with $\alpha = 0.05$ and $\alpha = 0.01$. The Ljung-Box Q-test statistic (Q-stat) #lags=log(sample size); *,**, and *** indicate rejection of H_0 of white noise at 5%, 1% and 0.1% level of significance respectively. 01/01/1999 through 02/01/2007 sample period.

Table 2: Subsample summary statistics for realized volatility jumps in JPY/USD exchange rate

	High Differential		Low Differential		High VIX		Low VIX	
	$\kappa_-(\alpha=0.01)$	$\kappa_+(\alpha=0.01)$	$\kappa_-(\alpha=0.01)$	$\kappa_+(\alpha=0.01)$	$\kappa_-(\alpha=0.01)$	$\kappa_+(\alpha=0.01)$	$\kappa_-(\alpha=0.01)$	$\kappa_+(\alpha=0.01)$
Prop.	10.51%	10.90%	6.69%	8.12%	9.34%	5.80%	7.83%	8.58%
Obs.	278	286	177	213	247	152	207	225
Mean	0.124	0.093	0.093	0.109	0.140	0.099	0.078	0.082
St. Dev.	0.160	0.089	0.113	0.098	0.177	0.126	0.080	0.107
Skew.	3.941	2.976	5.172	2.906	3.769	5.074	2.672	5.765
Kurt.	23.883	17.218	42.683	15.898	20.888	35.761	11.442	48.260
Min.	0.002	0.001	0.002	0.001	0.002	0.003	0.002	0.007
Max.	1.386	0.780	1.124	0.780	1.386	1.125	0.510	1.125
Q-stat	88.506***	1.399	46.481***	1.253	63.216***	4.708	25.4126***	3.616

Note: Jumps with $\alpha = 0.01$. The Ljung-Box Q-test statistic (Q-stat) #lags=log(sample size); *,**, and *** indicate rejection of H_0 of white noise at 5%, 1% and 0.1% level of significance respectively. 01/01/1999 through 02/01/2007 sample period.

Table 3: DBS test for non-linear dependence in realized volatility jumps

	Yen Appreciation Jumps						**Yen Deprectiation Jumps**					
	κ-		*κ-(α=0.05)*		*κ-(α=0.01)*		*κ+*		*κ+(α=0.05)*		*κ+(α=0.01)*	
Dim. (m)	BDS-stat	p-value	BDS-stat	p-value	BDS-stat	p-value	BDS-stat	p-value	BDS-stat	p-value	BDS-stat	p-value
2	0.024***	0.000	0.015***	0.000	0.008**	0.016	0.009***	0.000	0.002	0.554	0.005	0.144
	(0.003)		(0.003)		(0.003)		(0.003)		(0.003)		(0.004)	
3	0.043***	0.000	0.025***	0.000	0.016***	0.008	0.017***	0.000	0.002	0.698	0.007	0.222
	(0.004)		(0.005)		(0.006)		(0.004)		(0.005)		(0.006)	
4	0.055***	0.000	0.028***	0.000	0.022***	0.002	0.019***	0.000	0.001	0.85	0.007	0.278
	(0.005)		(0.006)		(0.007)		(0.005)		(0.006)		(0.007)	
5	0.063***	0.000	0.029***	0.000	0.022***	0.006	0.020***	0.000	0.002	0.73	0.007	0.3
	(0.005)		(0.006)		(0.007)		(0.005)		(0.006)		(0.007)	
6	0.065***	0.000	0.027***	0.000	0.020***	0.010	0.021***	0.000	0.002	0.622	0.004	0.49
	(0.005)		(0.006)		(0.007)		(0.005)		(0.006)		(0.007)	

Note: Standard erros in parenthesis; *,**, and *** indicate rejection of the null of I.I.D. at 5%, 1% and 0.1% level of significance respectively Test parametrized to be most parsimonious to unknown distribution in the data so acceptance parameter selected such that 0.7 of the total number of pairs of points in the sample lie within the acceptance radius and p-values calculated by bootstrapping based on 1,000 repetitions. Embeding dimention (m) chosed as log(sample size) of the data.

Table 4: Parameter estimates for the tail in the distribution of yen appreciation jumps

κ-			***κ-(α=0.05)***			***κ-(α=0.01)***		
Exp-PL	Pareto	Lognorm	Exp-PL	Pareto	Lognorm	Exp-PL	Pareto	Lognorm
ζ	ζ	μ	ζ	ζ	μ	ζ	ζ	μ
3.110	3.183	-0.776	2.377	2.615	-1.618	2.246	2.704	-1.501
(0.193)	(0.258)	(0.056)	(0.199)	(0.207)	(0.041)	(0.204)	(0.223)	(0.048)
φ		σ	φ		σ	φ		σ
0.080		0.463	0.528		0.564	1.040		0.528
(0.021)		(0.040)	(0.018)		(0.029)	(0.023)		(0.034)
loglike	loglike	loglike	loglike	loglike	loglike	loglike	loglike	loglike
39.012	38.993	9.387	209.283	208.458	146.591	128.253	127.16	89.24
AIC	AIC	AIC	AIC	AIC	AIC	AIC	AIC	AIC
-74.024	-75.986	-14.774	-414.566	-414.916	-289.182	-252.506	-252.320	-174.480
AICc	AICc	AICc	AICc	AICc	AICc	AICc	AICc	AICc
-73.845	-75.898	-14.595	-414.502	-414.884	-289.118	-252.406	-252.270	-174.380
Cutoff:	0.291		Cutoff:	0.107		Cutoff:	0.124	
	(0.051)			(0.033)			(0.027)	
Tail Obs.	70		Tail Obs.	190		Tail Obs.	123	
	(141.455)			(57.801)			(40.092)	
Obs.	1,255		Obs.	650		Obs.	455	

Note: The power exponent estimated via the maximum likelihood then select the minimum cutoff κ that gives the minimum KS-statistic. Standrad errors for ζ and φ calculated using Bayesian MCMC method based on 10,000 simulations.

Table 5: Parameter estimates for the tail in the distribution of yen depreciation jumps

κ_+			$\kappa_+(\alpha=0.05)$			$\kappa_+(\alpha=0.01)$		
Exp-PL	Pareto	Lognorm	Exp-PL	Pareto	Lognorm	Exp-PL	Pareto	Lognorm
ζ	ζ	μ	ζ	ζ	μ	ζ	ζ	μ
2.51	2.967	-1.502	2.928	3.065	-1.538	2.983	3.229	-1.547
(0.202)	(0.224)	(0.036)	(0.203)	(0.286)	(0.045)	(0.203)	(0.395)	(0.047)
φ		σ	φ		σ	φ		σ
1.125		0.466	0.321		0.475	0.642		0.435
(0.018)		(0.026)	(0.026)		(0.032)	(0.032)		(0.034)
loglike	loglike	loglike	loglike	loglike	loglike	loglike	loglike	loglike
198.864	197.884	142.702	145.335	145.234	99.382	117.424	117.284	84.037
AIC	AIC	AIC	AIC	AIC	AIC	AIC	AIC	AIC
-393.728	-393.768	-281.404	-286.670	-288.468	-194.764	-230.848	-232.568	-164.074
AICc	AICc	AICc	AICc	AICc	AICc	AICc	AICc	AICc
-393.549	-393.680	-281.225	-286.606	-288.436	-194.700	-230.748	-232.518	-163.974
Cutoff:	0.134		Cutoff:	0.132		Cutoff:	0.136	
	(0.030)			(0.034)			(0.035)	
Tail Obs.	168		Tail Obs.	115		Tail Obs.	87	
	(111.917)			(74.413)			(64.540)	
Obs.	1,276		Obs.	628		Obs.	438	

Note: The power exponent estimated via the maximum likelihood then select the minimum cutoff κ that gives the minimum KS-statistic. Standrad errors for ζ and φ calculated using Bayesian MCMC method based on 10,000 simulations.

Table 6: Exponentially dampened power-law parameter estimates (tail cutoff at 1 s.d.)

	Yen Appreciation Jumps			**Yen Depreciation Jumps**		
	κ_-	$\kappa_-(\alpha=0.05)$	$\kappa_-(\alpha=0.01)$	κ_+	$\kappa_+(\alpha=0.05)$	$\kappa_+(\alpha=0.01)$
ζ	2.288	2.23	1.527	2.146	2.049	1.495
	(0.197)	(0.196)	(0.201)	(0.200)	(0.200)	(0.201)
φ	0.713	0.744	2.48	1.858	1.992	4.324
	(0.026)	(0.035)	(0.041)	(0.028)	(0.039)	(0.046)
Cutoff:	0.113	0.097	0.073	0.079	0.068	0.055
Loglike.	286.25	237.038	244.226	538.233	428.577	421.284
Tail Obs.	274	211	210	368	283	268
Obs.	1255	650	455	1276	628	438

Note: Exponentially dampened power-law parameters re-estimated expanding the tails of the distribution to 1 S.D. bounds.

Table 7: Distribution paremeter estimates, sample split by interest rate differential.

High Differential						**Low Differential**					
κ-(α=0.01)			κ_+(α=0.01)			κ-(α=0.01)			κ_+(α=0.01)		
Exp-PL	Pareto	Lognorm	Exp-PL	Pareto	Lognorm	Exp-PL	Pareto	Lognorm	Exp-PL	Pareto	Lognorm
ζ	ζ	μ	ζ	ζ	μ	ζ	ζ	μ	ζ	ζ	μ
2.007	2.569	-1.530	2.769	3.610	-1.461	2.394	2.874	-1.785	2.894	2.932	-1.745
(0.194)	(0.406)	(0.057)	(0.200)	(0.690)	(0.052)	(0.204)	(0.511)	(0.065)	(0.198)	(0.439)	(0.081)
φ		σ	φ		σ	φ		σ	φ		σ
1.250		0.561	2.408		0.355	1.410		0.487	0.094		0.531
(0.060)		(0.041)	(0.100)		(0.038)	(0.106)		(0.047)	(0.114)		(0.059)
loglike	loglike	loglike	loglike	loglike	loglike	loglike	loglike	loglike	loglike	loglike	loglike
92.538	93.749	65.281	68.830	68.576	51.153	78.550	81.079	61.272	63.659	63.671	42.640
Cutoff:	0.1138		Cutoff:	0.1568		Cutoff:	0.0975		Cutoff:	0.1029	
	(0.063)			(0.049)			(0.031)			(0.024)	
Tail Obs.	94		Tail Obs.	48		Tail Obs.	56		Tail Obs.	44	
	(46.707)			(55.433)			(32.467)			(21.661)	
Obs.	278		Obs.	286		Obs.	177		Obs.	152	

Note: The power exponent estimated via the maximum likelihood then select the minimum cutoff κ that gives the minimum KS-statistic. Standrad errors for ζ and φ calculated using Bayesian MCMC method based on 10,000 simulations. Sample split into jumps associated with the interest rate differential above and below 2%.

Table 8: Distribution paremeter estimates, subsample split by VIX.

High VIX						**Low VIX**					
κ-(α=0.01)			κ_+(α=0.01)			κ-(α=0.01)			κ_+(α=0.01)		
Exp-PL	Pareto	Lognorm	Exp-PL	Pareto	Lognorm	Exp-PL	Pareto	Lognorm	Exp-PL	Pareto	Lognorm
ζ	ζ	μ	ζ	ζ	μ	ζ	ζ	μ	ζ	ζ	μ
2.358	2.664	-1.466	2.719	3.398	-1.539	1.933	2.682	-2.131	2.885	3.035	-1.590
(0.190)	(0.212)	(0.059)	(0.198)	(0.558)	(0.053)	(0.198)	(0.324)	(0.056)	(0.196)	(0.333)	(0.086)
φ		σ	φ		σ	φ		σ	φ		σ
0.620		0.564	1.999		0.387	3.327		0.526	0.223		0.509
(0.060)		(0.043)	(0.098)		(0.039)	(0.099)		(0.040)	(0.120)		(0.063)
loglike	loglike	loglike	loglike	loglike	loglike	loglike	loglike	loglike	loglike	loglike	loglike
88.777	88.323	55.604	77.050	76.759	57.142	142.520	144.235	117.057	45.868	48.614	30.994
Cutoff:	0.1257		Cutoff:	0.1403		Cutoff:	0.0651		Cutoff:	0.1231	
	(0.019)			(0.037)			(0.019)			(0.025)	
Tail Obs.	90		Tail Obs.	53		Tail Obs.	86		Tail Obs.	36	
	(17.934)			(36.537)			(23.712)			(34.358)	
Obs.	248		Obs.	213		Obs.	207		Obs.	225	

Note: The power exponent estimated via the maximum likelihood then select the minimum cutoff κ that gives the minimum KS-statistic. Standrad errors for ζ and φ calculated using Bayesian MCMC method based on 10,000 simulations. Sample split into jumps associated with the VIX above and below 20 points.

Table 9: MCMC estimation results of the linear coeffients of tail exponential truncation parameter ϕ on $(i-i^*)$ and the VIX

Parameter:	φ_-		φ_+	
	(1)	(2)	(1)	(2)
(i-i*)	-1.676 **		-1.701 **	
	(0.718)		(0.689)	
MC S.E	0.076		0.025	
VIX		-1.838 ***		-1.720 ***
		(0.581)		(0.571)
MC S.E		0.026		0.022
τ_ε	0.911	0.743	0.829	0.764
	(0.764)	(0.601)	(0.568)	(0.516)
MC S.E	0.130	0.053	0.042	0.040

Note: Results based on 10,000 samples after discarding the first 4,000 iterations as "burn-in". Standard errors in parenthesis. *, **, and *** indicate coefficientes significant at 10%, 5%, and 1% level respectively under the normality assumption for the simulated parameter values.

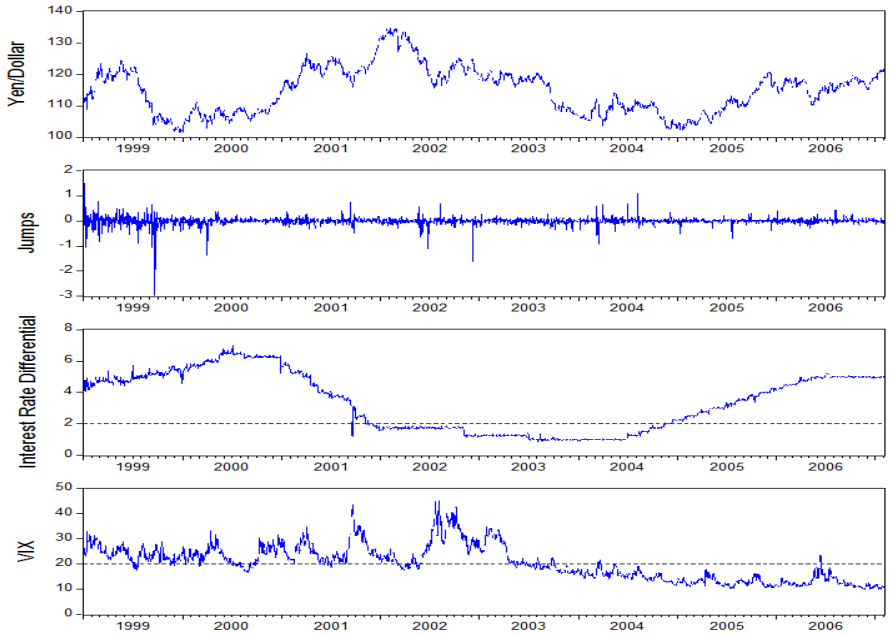

Figure 1: Daily time series of JPY/USD exchange rate, realized volatility jumps, U.S.-Japan interest rate differential, and CBOE VIX; 01/01/1999 through 02/01/2007 sample period.

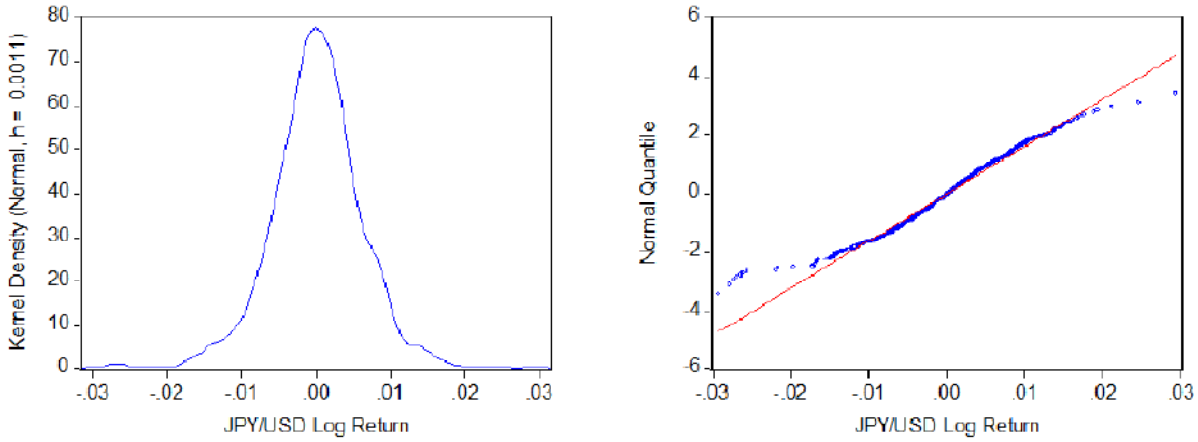

Figure 2: Distribution of JPY/USD Log Returns. *Left:* Kernel density; *Right:* Q-Q plot versus normal distribution

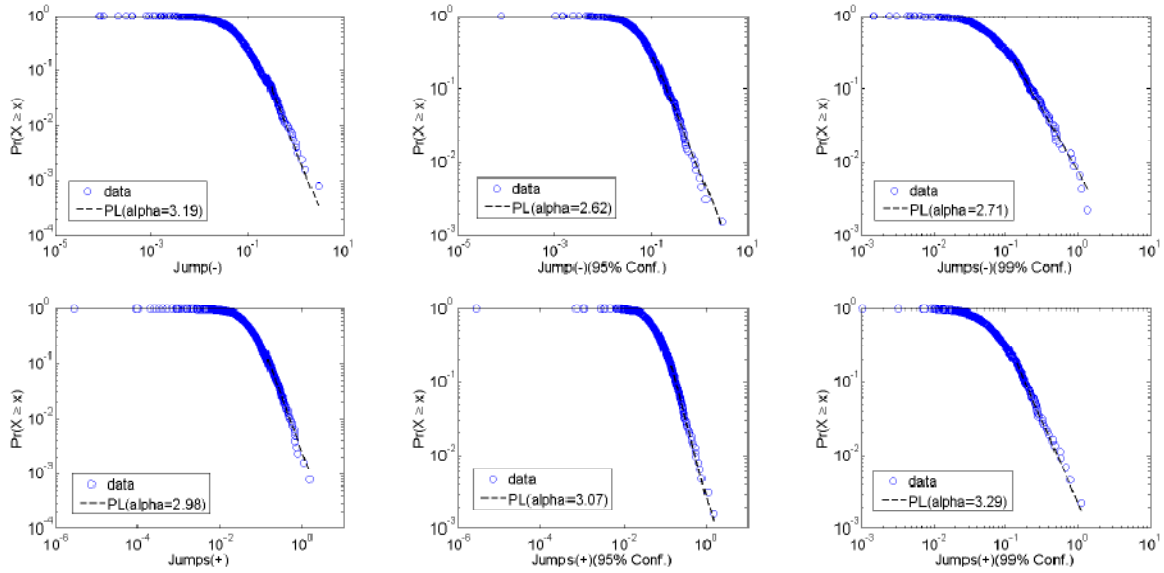

Figure 3: Power-law fits to the tail of realized volatility jump distribution, MLE method. *Top:* Yen appreciation jumps; *Bottom:* Yen depreciation jumps

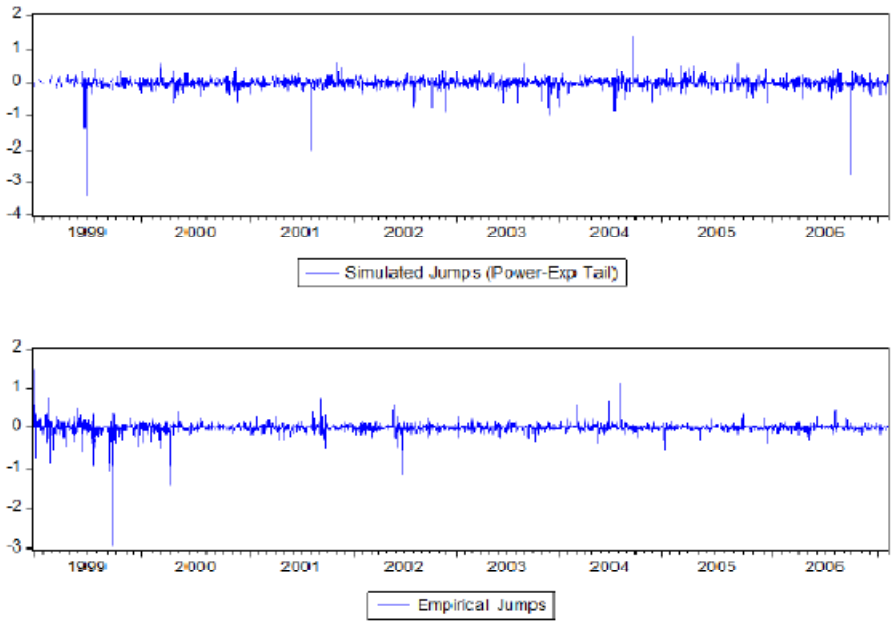

Figure 4: *Top:* Jumps in JPY/USD simulated using exponentially dampened power-law with parameters tail cutoff=0.124, ζ =2.246, ϕ=1.040 for κ_- and tail cutoff=0.136, ζ =2.983, ϕ=0.642 for κ_+; *Bottom:* Empirical realized volatility jumps series

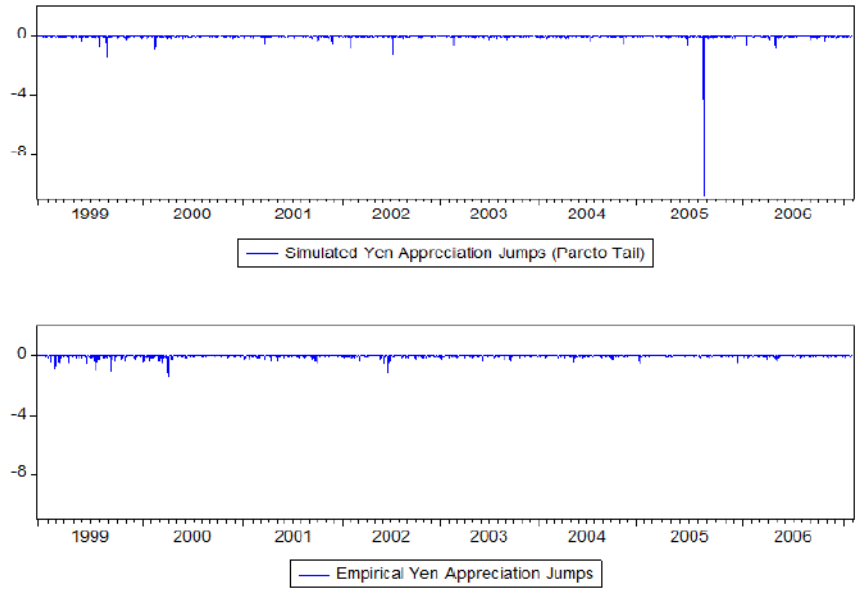

Figure 5: *Top:* Jumps in JPY/USD simulated using pure power-law with parameters tail cutoff=0.124, ζ =2.704; *Bottom:* empirical realized volatility jump series.

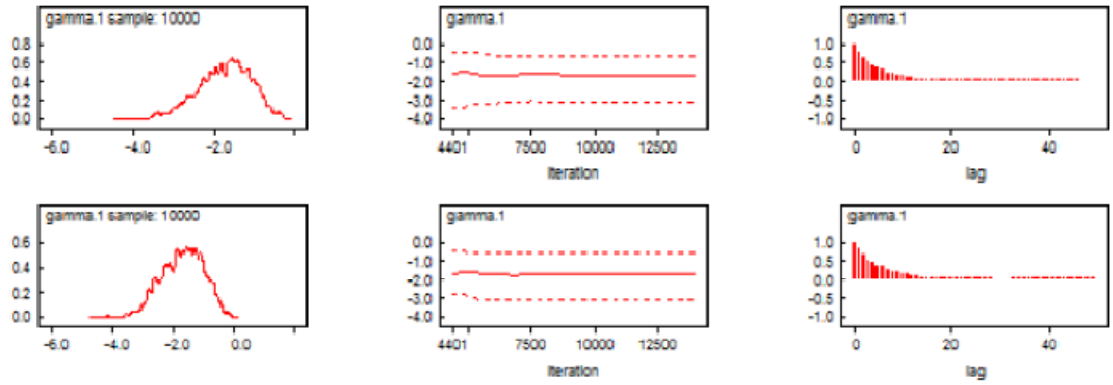

Figure 6: MCMC simulated coefficient on U.S.-Japan intererest rate differential: density plot, iterative quantile plot, and ACF. *Top:* exponential truncation in the negative tail of jump distribution, ϕ_-; *Bottom:* exponential truncation in the positive tail of jump distribution, ϕ_+

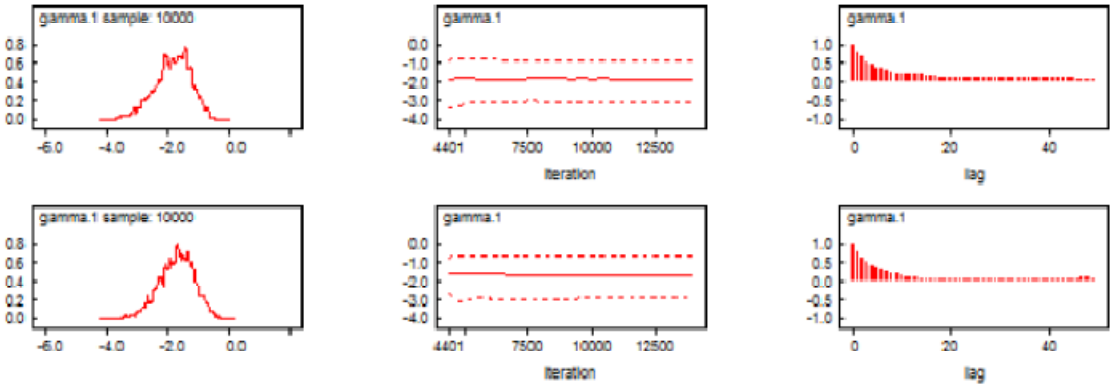

ccc

Figure 7: MCMC simulated coefficient on VIX: density plot, iterative quantile plot, and ACF. *Top:* exponential truncation in the negative tail of jump distribution, ϕ_-; *Bottom:* exponential truncation in the positive tail of jump distribution, ϕ_+